ENSTA Bretagne · Ifremer
15ÈMES JOURNÉES DE L'HYDRODYNAMIQUE
22 - 24 novembre 2016 - Brest

EVALUATION PRATIQUE DE LA RESISTANCE D'UN MONOCOQUE

PRACTICAL ESTIMATION OF THE DRAG OF A FREELY-FLOATING MONOHULL SHIP

Chao Ma[1], Francis Noblesse[1], Wei Li[1], Fuxin Huang[2], Chi Yang[2]

[1] Shanghai Jiao Tong University, Shanghai, China
[2] School of Physics, Astronomy & Computational Sciences, George Mason University, Fairfax VA, USA

Chao Ma: chaoma1988dr@163.com, Francis Noblesse: noblfranc@gmail.com

Résumé

Une méthode simple pour estimer l'assiette, le gîte et la résistance d'un navire monocoque à des nombres de Froude $F \leq 0.45$ est présentée. L'assiette et le gîte sont déterminés de deux manières alternatives: une approche expérimentale fondée sur une analyse de mesures données dans la literature, et une approche numérique fondée sur l'approximation potentielle linaire. L'assiette et le gîte sont determinés par des relations analytique simples, et donc sans calculs d'écoulement, dans l'approche expérimentale. L'approche numérique n'exige que des calculs d'écoulement autour de la carène Σ_0^H du navire au repos. Les deux approches donnent des prédictions raisonnables de l'assiette et du gîte pour un large éventail de monocoques. La résistance est aussi déterminée de manière simple, fondée sur la décomposition classique de Froude: des relations analytiques classiques sont utilisées pour la composante de viscosité, et la résistance de vagues est évaluée par la théorie (linaire potentielle) de Neumann-Michell. La résistance est plus sensible à la position du navire que l'assiette et le gîte, et doit donc être évaluée pour une carène 'dynamique' Σ_{st}^H qui rend compte de l'assiette et du gîte du navire. Cependant, il n'est pas necessaire que la carène Σ_{st}^H soit déterminée de manière trés précise. En fait, les carènes Σ_1^H et Σ_a^H obtenues au moyen de l'approche numérique ou de l'approche expérimentale ont des résistances pratiquement identiques. Par contre, la résistance de la carène Σ_1^H et la résistance (quasiment identique) de la carène Σ_a^H sont nettement plus élevées, et aussi en bien meilleur accord avec les mesures expérimentales, que la résistance de la carène Σ_0^H du navire au repos aux grands nombres de Froude.

Summary

A practical method for estimating the sinkage, the trim and the drag of a freely-floating common monohull ship at moderate Froude numbers $F \leq 0.45$ is considered. This method can be used for ship models as well as full-scale ships with smooth or rough hull surfaces, and is well suited for early ship design and hull form optimization. The sinkage and the trim are estimated via two alternative simple methods: an experimental approach based on experimental data given in the literature, and a numerical approach based on a practical linear potential-flow theory (the Neumann-Michell theory) that only requires simple flow computations. The experimental approach yields particularly simple analytical relations for the sinkage and the trim, and thus requires no flow computations. The numerical approach only involves flow computations for the hull surface Σ_0^H of the ship in equilibrium position at rest. Both approaches yield reasonable sinkage and trim predictions for a wide range of monohull ships. The drag is also estimated in a simple way, based on the classical Froude decomposition into viscous and wave components: well-known semiempirical expressions for the friction drag, the viscous drag and the drag due to hull roughness are used, and the wave drag is evaluated via the Neumann-Michell theory. The drag is more sensitive to the hull position than the sinkage and the trim. Accordingly, it must be computed for a 'dynamic' ship hull surface Σ_{st}^H that accounts for sinkage and trim effects, although the hull surface Σ_{st}^H does not need to be very precise. In fact, the hull surfaces Σ_1^H and Σ_a^H predicted by by the numerical approach or the experimental approach have nearly identical drags. However, the drag of the hull surface Σ_1^H and the (nearly identical) drag of the hull surface Σ_a^H are significantly higher, and also much closer to experimental measurements, than the drag of the hull surface Σ_0^H of the ship at rest at high Froude numbers.

1. Introduction

The drag experienced by a ship is a critical element of ship design. Accordingly, the prediction of the flow around a ship hull that advances at a constant speed along a straight path, in calm water of large depth and lateral extent, is a classical basic ship hydrodynamics problem that has been widely considered in a huge body of literature. Indeed, a number of alternative methods — including viscous flow computational methods, nonlinear or linear potential flow methods, and analytical methods — have been developed to compute the flow around a ship hull. A brief review of these alternative methods can be found in e.g. Noblesse et al. (2013a).

The drag of a ship is well known to be influenced by several complicated flow features, including (i) flow separation at a ship stern, notably a transom stern, (ii) wavebreaking at a ship bow, (iii) hull roughness for full-scale ships, and (iv) influence of sinkage and trim for a freely floating ship.

This study considers the influence of sinkage and trim on the drag of a common generic freely floating ship (free to sink and trim) at a moderate Froude number

$$F \equiv V/\sqrt{gL} \leq 0.45 \tag{1}$$

where V and L denote the speed and the length of the ship, and g is the acceleration of gravity. The analysis of sinkage and trim effects on the drag evidently involves two basic elements: the determination of sinkage and trim, and the determination of the drag. These two basic tasks are considered here via practical methods suited for routine applications to design.

1.1. Practical determination of sinkage and trim

The pressure distribution around a ship hull surface Σ^H that advances at a constant speed V in calm water evidently differs from the hydrostatic pressure distribution around the wetted hull surface Σ_0^H of the ship at rest, i.e. at zero speed $V = 0$. Consequently, the ship experiences a hydrodynamic lift and pitch moment, and a related vertical displacement and rotation of Σ_0^H that are commonly called sinkage and trim, and have been widely considered in the literature; e.g. Subramani et al. (2000), Yang et al. (2000, 2007), Yang & Löhner (2002), Ni et al. (2011), Yao & Dong (2012), He et al. (2015), Doctors (2015), Chen et al. (2016), Ma et al. (2016a). The differences between the wetted hull surface Σ_0^H of a ship at rest and the corresponding actual mean wetted ship hull surface Σ^H are illustrated in Fig.1 for three freely floating ship models at a Froude number $F = 0.4$.

As already noted, alternative methods for evaluating the sinkage and the trim, as well as the drag, experienced by a freely floating ship have been considered in the literature. In particular, the approach considered in Subramani et al. (2000), Yang et al. (2000), Yang & Löhner (2002), Ni et al. (2011), Yao & Dong (2012), He et al. (2015), Chen et al. (2016) involve iterative flow computations for a sequence of hull positions. Such iterative flow computations are not well suited for routine practical applications to early ship design and hull form optimization, and are shown in Ma et al. (2016a) to be unnecessary for typical monohull ships at Froude numbers $F \leq 0.45$. Practical methods for estimating the sinkage, the trim and the drag of a ship, notably methods that do not require iterative flow computations for a sequence of hull positions, are useful if not necessary at early design stages and for hull form optimization.

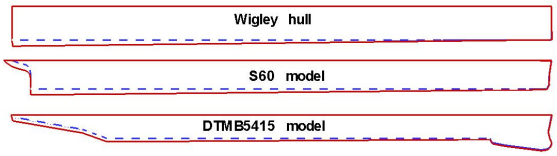

Figure 1: Profiles of the wetted hull surfaces of the Wigley hull, the S60 model and the DTMB5415 model at rest (blue dashed lines) and in freely floating positions at Froude numbers $F = 0.4$ (red solid lines).

Ma et al. (2016a) considers two simple approaches, an 'experimental approach' and a 'numerical approach', for estimating the sinkage and the trim of a typical freely floating monohull ship that advances in deep water at a Froude number $F \leq 0.45$.

The experimental approach is based on an analysis of experimental measurements reported in the literature for 22 models of monohull ships. This analysis of experimental data yields particularly simple approximate analytical relations that explicitly (without flow computations) predict the sinkage and the trim experienced by a monohull ship in terms of the ship speed V and four main hull-geometry parameters: the length L, the beam B, the draft D, and the block coefficient C_b.

The numerical approach only involves linear potential flow computations for the ship at rest, i.e. for the wetted hull surface Σ_0^H, rather than for the mean wetted hull surface Σ^H of the ship at its actual position. Indeed, a main conclusion of Ma et al. (2016a) is that, for common monohull ships at Froude numbers $F \leq 0.45$, the sinkage and the trim can be realistically predicted via computations for the 'static' hull surface Σ_0^H of the ship at rest, i.e. without iterative flow computations for several hull positions. This practical simplification stems from the fact that the sinkage and the trim are mostly determined by the pressure distribution over the lower part of the ship hull surface, and consequently are not highly sensitive to the precise position of the ship. A linear potential flow method is used in the numerical approach considered in Ma et al. (2016a).

Both the simple numerical approach and the even simpler experimental approach are found in Ma et al. (2016a) to yield realistic overall predictions of sinkage and trim for a wide range of monohull ships at Froude numbers $F \leq 0.45$.

The influence of sinkage and trim on the drag of a typical monohull ship at a Froude number $F \leq 0.45$ is examined here, as already noted. The drag of a freely floating ship hull can be significantly larger than the drag of the hull surface Σ_0^H of the ship at rest, as well documented in the literature; e.g. Subramani et al. (2000),

Yang et al. (2000), Ni et al. (2011) and Ma et al. (2016b). For instance, the theoretical predictions reported in Ma et al. (2016b) show that at a Froude number $F = 0.45$, the Wigley hull and the S60 model experience an increase in total drag of about 15%, while the total drag of the DTMB5415 model is about 7% higher, due to sinkage and trim effects. These examples show that sinkage and trim effects on the drag of a ship (especially the wave drag component) can be significant and cannot be ignored, and moreover depend on the hull form. Thus, sinkage and trim effects on the drag need to be considered within the design process, arguably even at early design stages and for hull form optimization.

1.2. Practical determination of the drag

As required for routine applications to early ship design, and in accordance with the simple approaches considered in Ma et al. (2016a) for estimating the sinkage and the trim, a practical approach is also used in Ma et al. (2016b) to determine the drag of a typical freely floating monohull ship at Froude numbers $F \leq 0.45$. Specifically, classical semiempirical relations for the friction drag, the viscous drag and the drag due to hull roughness are used, and the wave drag is evaluated via a practical linear potential flow method. As is explained further on, the drag is much more sensitive to the hull position than the sinkage and the trim. Indeed, the drag must be computed for a 'dynamic' ship hull surface Σ^H_{st} that accounts for sinkage and trim effects.

However, the hull surface Σ^H_{st} does not need to be very precise. In fact, a notable result of the numerical computations given in Ma et al. (2016b) is that the total drag computed for a hull surface Σ^H_{st} chosen as the hull surface Σ^H_1 that is predicted by the numerical approach, i.e. potential flow computations for the hull surface Σ^H_0 of the ship at rest, or as the hull surface Σ^H_a that is predicted by the even simpler experimental approach, are nearly identical.

Moreover, the drag of the hull surface Σ^H_1 and the (nearly identical) drag of the hull surface Σ^H_a are significantly higher — and also much closer to experimental measurements for the Wigley, S60 and DTMB5415 models — than the drag of the hull surface Σ^H_0 of the ship at rest at high Froude numbers F (within the constraint $F \leq 0.45$ considered here). These numerical results suggest that sinkage and trim effects, significant at Froude numbers $0.35 \leq F$, on the drag of a typical freely floating monohull ship can be well accounted for in a practical way that only requires linear potential flow computations, without iterative computations for a sequence of hull positions.

1.3. Basic notations

Hereafter, coordinates and flow variables are made nondimensional in terms of the gravitational acceleration g, the water density ρ, and the length L and the speed V of the ship. The Cartesian system of nondimensional coordinates

$$(x, y, z) \equiv \mathbf{x} \equiv \mathbf{X}/L$$

is attached to the moving ship. The x axis is chosen along the path of the ship and points toward the ship bow. The undisturbed free surface is taken as the plane $z = 0$ and the z axis points upward. The ship bow and stern are located at $\mathbf{x}_b = (0.5, 0, 0)$ and at $\mathbf{x}_s = (-0.5, 0, 0)$. The unit vector

$$\mathbf{n} \equiv (n^x, n^y, n^z)$$

is normal to the hull surface Σ^H and points outside the ship (into the water).

The present study summarizes the analysis and the main results of the practical approaches considered in Ma et al. (2016a) and Ma et al. (2016b) for estimating the sinkage and the trim, and their influence on the drag, for a common freely-floating monohull ship at moderate Froude numbers $F \leq 0.45$.

2. Basic relations for the sinkage and the trim

Hereafter, the vertical displacement of a ship hull surface Σ^H from its position Σ^H_0 at rest, at midship, is called 'midship sinkage' and denoted as H^m. Similarly, the vertical displacement of Σ^H at the ship bow and stern are denoted as H^b and H^s, and called 'bow sinkage' and 'stern sinkage'. Positive values of H^m, H^b or H^s correspond to downward vertical displacements of Σ^H at midship, at a ship bow or at a ship stern, respectively. The rotation of Σ^H from Σ^H_0 is defined by the trim angle $\tau^\circ \equiv \tau^{rad}\, 180/\pi$ where the angles τ° and τ^{rad} are measured in degrees or in radians, or by the equivalent 'trim sinkage' H^τ defined as

$$2\, H^\tau \equiv L \tan(\tau^{rad}) \approx L\, \tau^{rad} \equiv L\, \tau^\circ \pi/180 \tag{2}$$

Positive values of τ°, τ^{rad}, H^τ correspond to a bow-up rotation.

The relations

$$H^s = H^m + H^\tau \;\text{ and }\; H^b = H^m - H^\tau \tag{3}$$

hold. These geometrical identities determine the stern sinkage H^s and the bow sinkage H^b from the midship sinkage H^m and the trim sinkage H^τ that are computed in the numerical approach considered in section 3. The relations (3) readily yield

$$H^b = 2H^m - H^s \;\text{ and }\; H^\tau = H^s - H^m \tag{4}$$

These relations determine the bow sinkage H^b and the trim sinkage H^τ from the midship sinkage H^m and the stern sinkage H^s that are determined in section 4 by simple analytical relations obtained via an analysis of experimental measurements.

3. Numerical determination of sinkage and trim

The midship sinkage H^m and the trim sinkage H^τ, where a positive sinkage $0 < H^m$ or a positive trim sinkage $0 < H^\tau$ correspond to a downward vertical displacement or a bow-up rotation of the ship hull as already noted, are determined via the relations

$$\frac{H^m/L}{F^2} \approx \frac{C^z + \varepsilon_2\, C^{zx}}{a_0\,(1 - \varepsilon_0\, \varepsilon_2)} \text{ and } \frac{2\, H^\tau/L}{F^2} \approx \frac{C^{zx} + \varepsilon_0\, C^z}{a_2\,(1 - \varepsilon_0\, \varepsilon_2)} \tag{5a}$$

Here, $\varepsilon_0 \equiv a_1/a_0$ and $\varepsilon_2 \equiv a_1/a_2$. Moreover, a_0, a_1 and a_2 denote the nondimensional area of the waterplane W_0^H of the wetted hull surface Σ_0^H and the related moments defined as

$$(a_0, a_1, a_2) \equiv \left(\frac{A_0}{L^2}, \frac{A_1}{L^3}, \frac{A_2}{L^4}\right) \equiv \int_{W_0^H} (1, x, x^2)\, dx\, dy \quad (5b)$$

The terms C^z and C^{zx} in (5a) represent the nondimensional hydrodynamic lift and moment coefficients defined as

$$(C^z, C^{zx}) = \int_{\Sigma^H} (n^z, n^x z - n^z x)\, p\, da \quad (5c)$$

where the hydrodynamic pressure p is determined by the Bernoulli relation

$$p = \sqrt{(n^y)^2 + (n^z)^2}\, \phi_t + (n^x)^2/2 - (\phi_t^2 + \phi_d^2)/2 \quad (5d)$$

Here, $\phi_t \equiv \partial\phi/\partial t$ and $\phi_d \equiv \partial\phi/\partial d$ denote the velocity components along two unit vectors $\mathbf{t}$ and $\mathbf{d}$ tangent to the ship hull surface Σ^H. These tangential velocity components are evaluated here via the Neumann-Michell (NM) theory expounded in Noblesse et al. (2013a), Huang et al. (2013) and Noblesse et al. (2013b).

The nondimensional hydrodynamic lift and pitch moment coefficients C^z and C^{zx} given by (5c) where the mean wetted ship hull surface Σ^H is taken as the static wetted hull surface Σ_0^H are denoted as C_0^z and C_0^{zx}. The midship sinkage H^m and the trim sinkage H^τ given by (5a) where C^z and C^{zx} are taken as C_0^z and C_0^{zx} are similarly denoted as H_0^m and H_0^τ. The mean wetted hull surface that is obtained from the wetted hull surface Σ_0^H of a ship at rest via a translation H_0^m and a rotation H_0^τ is denoted as Σ_1^H, and the hydrodynamic coefficients C^z and C^{zx} given by (5c) with Σ^H taken as Σ_1^H are denoted as C_1^z and C_1^{zx}. Similarly, H_1^m and H_1^τ denote the sinkage H^m and the trim H^τ determined from (5a) with C^z and C^{zx} taken as C_1^z and C_1^{zx}.

Expressions (5c) for C^z and C^{zx} show that, except for a ship hull with large flare and rake angles, the upper part of a ship hull (where $n^z \approx 0$) does not contribute appreciably to the sinkage, and that the upper hull and the parallel midbody (where $n^x z \approx 0$ and $n^z x \approx 0$) do not contribute much to the trim. Thus, the main contributions to the sinkage and the trim stem from the lower part of the ship hull surface. It can then be expected that the sinkage and the trim are relatively insensitive to the precise position of the ship hull, and can be realistically evaluated from the pressure at the hull surface Σ_0^H of the ship at rest. This theoretical expectation is confirmed in Fig.7, where the sinkage H^m and the trim H^τ computed for the hull surfaces Σ^H taken as Σ_0^H or Σ_1^H are compared.

4. Explicit relations for the sinkage and the trim

The previously-noted fact that the sinkage and the trim of a ship predominantly stem from the pressure distribution over the lower part of the ship hull surface also suggests that the sinkage and the trim may not be highly sensitive to 'details' of the hull form (such as a transom stern) and the Reynolds number, and might reasonably be assumed to primarily depend on the Froude number and basic hull form parameters (such as the beam/length ratio B/L and the block coefficient C_b) that characterize the overall hull geometry. This theoretical conjecture is considered in Ma et al. (2016a) via an analysis of experimental measurements of sinkage and trim for 22 models of freely-floating monohull ships.

Ship model	B/L	D/L	D/B	C_b	Symbol
USH-3b	0.144	0.071	0.500	0.397	+
USH-4a	0.096	0.064	0.667	0.397	□
USH-4b	0.111	0.056	0.500	0.397	+
USH-4c	0.125	0.050	0.400	0.397	✳
USH-5a	0.078	0.052	0.667	0.397	□
USH-5b	0.091	0.045	0.500	0.397	⊙
USH-5c	0.101	0.040	0.400	0.397	▼
USH-5d	0.091	0.045	0.500	0.396	◆
USH-5e	0.091	0.045	0.500	0.398	△
USH-6a	0.066	0.044	0.667	0.397	△
USH-6b	0.076	0.038	0.500	0.397	✳
USH-6c	0.085	0.034	0.400	0.397	✳
Wigley	0.100	0.063	0.625	0.445	+
S60	0.130	0.052	0.400	0.600	×
DTMB5415	0.134	0.043	0.323	0.510	✳
Delft372	0.080	0.050	0.625	0.403	⊙
ONRT	0.122	0.036	0.292	0.539	□
JHSS-BB	0.111	0.031	0.276	0.437	▼
JHSS-EB	0.111	0.031	0.276	0.437	◆
JHSS-GB	0.108	0.030	0.276	0.432	△
JHSS-ST	0.111	0.031	0.276	0.437	△
Model5365	0.148	0.033	0.226	0.438	✤

Table 1: Beam/length ratio B/L, draft/length ratio D/L, draft/beam ratio D/B and block coefficient C_b for the 22 ship models considered in the analysis of experimental measurements of sinkage and trim. The symbols that identify the 22 ship models in Figs.3-5 are also shown.

4.1. Experimental data base

Specifically, the experimental measurements of sinkage and trim for 22 models of monohull ships reported in Kajitani et al. (1983), McCarthy (1985), Molland et al. (1994, 1995), Olivieri et al. (2001), Fu et al. (2005), Cusanelli (2007), Cook (2011), Broglia et al.(2011, 2014), Souto-Iglesias et al. (2012) are analyzed in Ma et al. (2016a).

Table 1 shows that the beam/length ratio B/L, the draft/length ratio D/L, the draft/beam ratio D/B and the block coefficient C_b for these 22 ship models vary within the relatively broad ranges

$$0.066 \le B/L \le 0.148 \;,\; 0.029 \le D/L \le 0.071$$
$$0.276 \le D/B \le 0.667 \;,\; 0.397 \le C_b \le 0.6$$

These ranges of variations of B/L, D/L, D/B and C_b correspond to a fairly wide range of hull forms, as illustrated in Fig.2 for eight of the 22 ship models.

Fig.3 depicts the experimental measurements, for the Froude number F within the range $0.1 \le F \le 0.45$, of

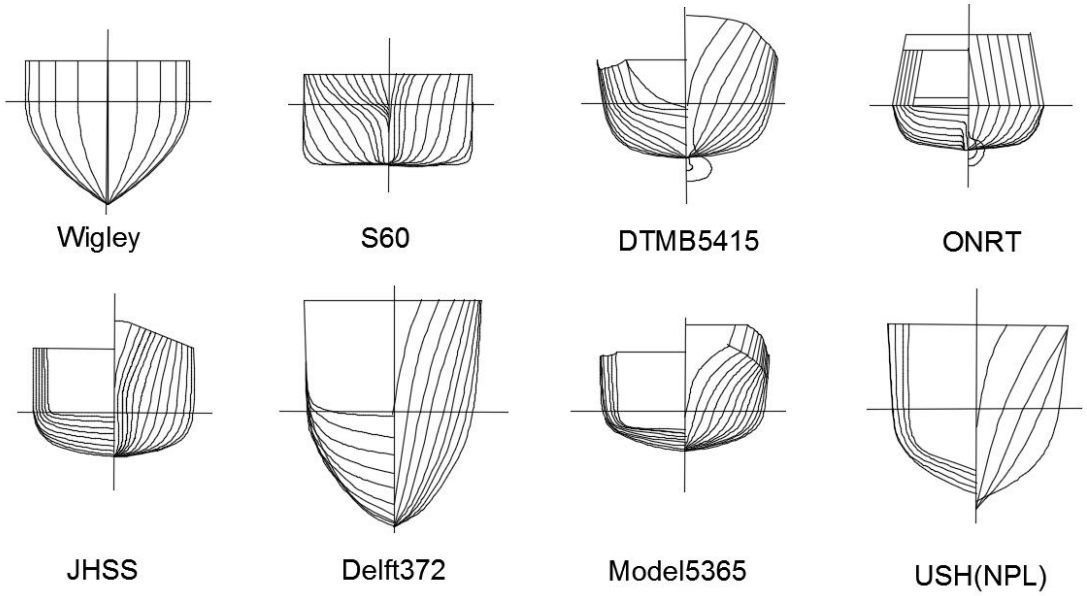

Figure 2: Framelines of 8 ship models in the series of 22 models considered in the analysis of experimental measurements of sinkage and trim.

the midship sinkage H^m, the trim sinkage H^τ, the stern sinkage H^s and the bow sinkage H^b — made nondimensional with respect to the ship draft D — for the 22 ship models. This figure shows that the midship sinkage H^m and the stern sinkage H^s mostly increase monotonically as the Froude number F increases. However, the variations of the trim sinkage H^τ and the bow sinkage H^b are more complicated. Accordingly, the experimental measurements of the midship sinkage H^m and the stern sinkage H^s are analyzed, and the bow sinkage H^b and the trim sinkage H^τ are determined from H^m and H^s via the geometrical relations (4). Fig.3 also shows that the trim sinkage H^τ and the stern sinkage H^s are small for Froude numbers smaller than about 0.3 but increase rapidly for $0.35 < F$. Indeed, the stern sinkage H^s can be as large as 35% of the ship draft D at $F = 0.45$.

4.2. Midship sinkage

The variations of the experimental measurements of the midship sinkage H^m for the 22 models of monohull ships depicted in the top left corner of Fig.3 with respect to the Froude number F and the four basic hull form parameters B/L, D/L, D/B and C_b are analyzed in Ma et al. (2016a). This analysis shows that the midship sinkage H^m increases approximately like F^2 as $F \leq 0.45$ increases, is approximately proportional to $\sqrt{BD}$, and moreover increases as the block coefficient C^b increases. Specifically, the detailed analysis of experimental measurements of the midship sinkage H^m given in Ma et al. (2016a) shows that H^m can be explicitly estimated in terms of the beam B, the draft D, the block coefficient C_b and the Froude number F via the analytical relation

$$H^m/\sqrt{BD} \approx F^2 C^m \quad \text{where} \quad C^m \equiv 0.9(C_b - 0.13) \tag{6}$$

The experimental measurements of $(H^m/\sqrt{BD})/C^m$ are depicted in Fig.4 for the 22 ship models. The thick solid (red) line and the two thick dashed (blue) lines in this figure correspond to the function F^2 or the functions $(1 \pm 0.3)F^2$, respectively. The two thin solid (black) lines that bound the shaded region correspond to the functions $(1 \pm 0.2)F^2$. Most of the experimental measurements are within the shaded region bounded by the two curves $(1 \pm 0.2)F^2$, and nearly all the measurements are between the two thick dashed (blue) curves $(1 \pm 0.3)F^2$. The simple analytical approximation (6) can then predict the midship sinkage H^m of a wide range of monohull ships with an accuracy of 20% in most cases and 30% in nearly all cases.

4.3. Stern sinkage

The variations of the experimental measurements of the stern sinkage H^s for the 22 models of monohull ships depicted in the bottom left corner of Fig.3 with respect to the Froude number F and the four basic hull form parameters B/L, D/L, D/B and C_b are analyzed in Ma et al. (2016a). This analysis shows that the stern sinkage H^s increases approximately like the function

$$f \equiv F_*^2\sqrt{1 + F_*^8} \quad \text{where} \quad F_* \equiv F/\,0.33 \tag{7a}$$

as $F \leq 0.45$ increases, and is approximately proportional to $\sqrt{BD}$. The available experimental measurements of H^s show no convincing correlations between H^s and C^b. Specifically, the detailed analysis of experimental measurements of the stern sinkage H^s given in Ma et al. (2016a) shows that H^s can be explicitly estimated in terms of the beam B, the draft D, and the Froude number F via the simple analytical relation

$$40\,H^s/\sqrt{BD} \approx f \tag{7b}$$

where f is defined by (7a).

The experimental measurements of $40\,H^s/\sqrt{BD}$ are depicted in Fig.5 for the 22 ship models. The thick solid (red) line and the two thick (blue) dashed lines in this figure correspond to the function $f \equiv F_*^2\sqrt{1+F_*^8}$ and

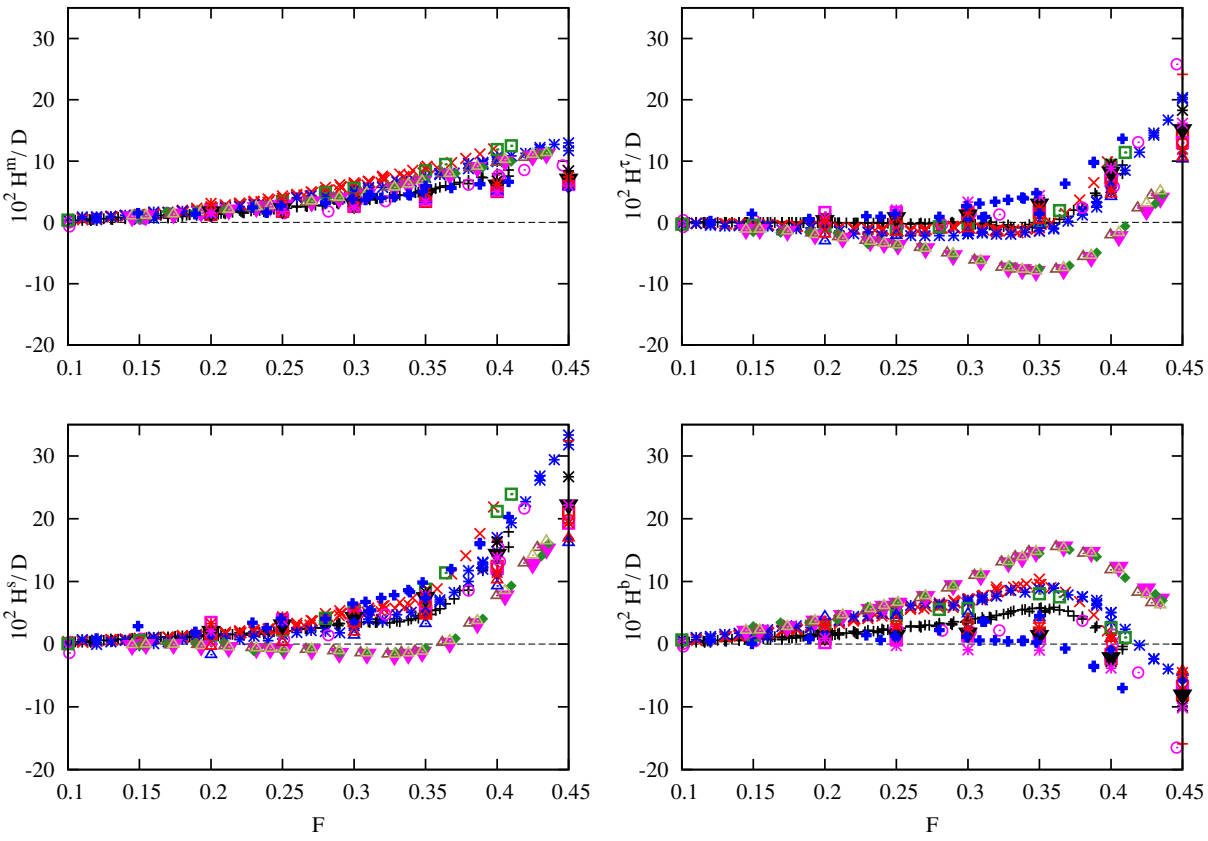

Figure 3: Midship sinkage H^m/D (top left corner), trim sinkage H^τ/D (top right), stern sinkage H^s/D (bottom left) and bow sinkage H^b/D (bottom right) for 22 models of monohull ships, identified by the symbols listed in Table 1, at $0.1 \le F \le 0.45$.

the functions $(1 \pm 0.4)f$, respectively. The two thin solid (black) lines that bound the shaded region correspond to the functions $(1 \pm 0.2)f$. The measurements are largely inside the shaded region, and most of the measurements are between the two thick dashed (blue) curves $(1\pm0.4)f$. The approximation (7) can then predict the stern sinkage H^s of a wide range of monohull ships with an accuracy of 20% in many cases and 40% in most cases.

4.4. Explicit analytical approximations

The midship sinkage H^m and the stern sinkage H^s can then be approximately determined by means of the simple analytical relations (6) and (7), and the bow sinkage H^b and the trim sinkage H^τ can be determined from H^m and H^s via the geometrical relations (4). Thus, the analysis of experimental measurements considered in Ma et al. (2016a) determines the midship sinkage H^m, the stern sinkage H^s, the bow sinkage H^b and the trim sinkage H^τ via the analytical relations

$$H^m \approx 0.9\,\sqrt{BD}\,(C_b - 0.13)F^2 \tag{8a}$$

$$H^s \approx 0.025\,\sqrt{BD}\,F_*^2\,\sqrt{1+F_*^8} \quad \text{with} \quad F_* \equiv F/0.33 \tag{8b}$$

$$H^b = 2H^m - H^s \quad \text{and} \quad H^\tau \equiv L\tau^\circ\pi/360 = H^s - H^m \tag{8c}$$

The trim angle τ° in (8c) is measured in degrees. The relations (8) determine H^m, H^s, H^b and H^τ in terms of the Froude number F and three major parameters — the beam B, the draft D, and the block coefficient C_b — that characterize the ship hull form. These relations explicitly determine the sinkage and the trim without flow computations, and are then particularly simple.

5. Practical determination of the drag

The nondimensional drag coefficient

$$C^t \equiv D/(\rho V^2 L^2) \tag{9}$$

is evaluated in Ma et al. (2016b) in a simple way, based on the classical Froude decomposition into viscous and wave components, as in Yang et al. (2013). Specifically, C^t is expressed as

$$C^t = C^w + C^v + C^a \tag{10}$$

where C^w represents the wave drag coefficient, C^v is the viscous drag coefficient for a smooth ship hull, and C^a accounts for the additional drag due to roughness.

The viscous drag C^v in (10) is expressed as

$$C^{\mathrm{v}} = (1+k)\,C^{\mathrm{f}} \tag{11a}$$

where C^{f} and k are the usual friction drag coefficient and form factor. The friction drag C^{f} is evaluated via the ITTC 1957 formula

$$C^{\mathrm{f}} = \frac{A^H}{2L^2}\,\frac{0.075}{(log_{10}R_e - 2)^2} \quad \text{where} \quad R_e \equiv \frac{VL}{\nu} \tag{11b}$$

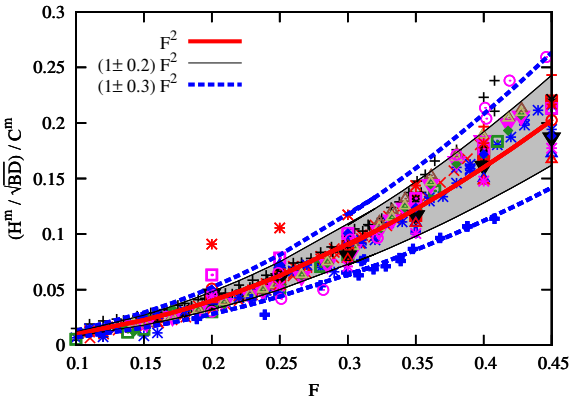

Figure 4: Variations of experimental measurements of $(H^m/\sqrt{BD})/C^m$ with $C^m \equiv 0.9(C_b - 0.13)$ with respect to the Froude number F for 22 ship models. The thick solid (red) line and the two thick dashed (blue) lines correspond to the function F^2 and the functions $(1 \pm 0.3)F^2$, respectively. The two thin solid (black) lines that bound the shaded region correspond to the functions $(1 \pm 0.2)F^2$.

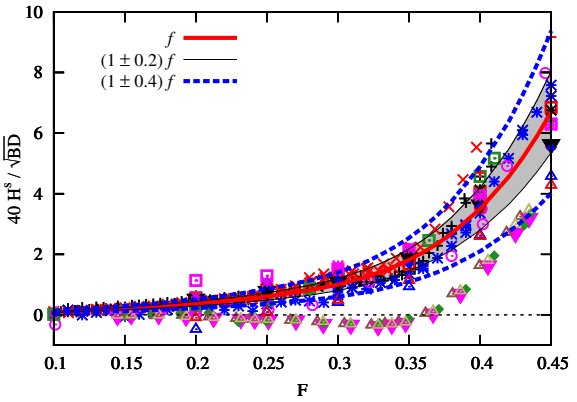

Figure 5: Variations of experimental measurements of $40\,(H^s/\sqrt{BD})$ with respect to the Froude number F for 22 ship models. The thick solid (red) line and the two thick dashed (blue) lines correspond to the function f and the functions $(1\pm0.4)f$, respectively. The two thin solid (black) lines that bound the shaded region correspond to the functions $(1 \pm 0.2)f$.

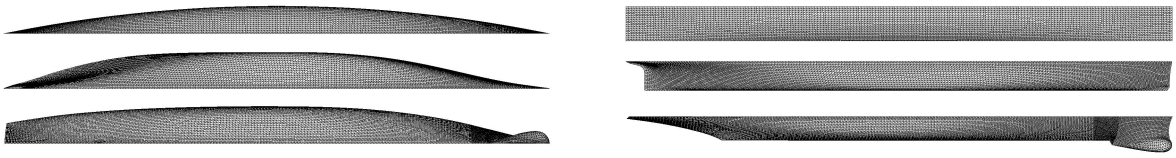

Figure 6: Side views (left) and bottom views (right) of the wetted hull surfaces Σ_0^H of the Wigley hull (top), the S60 model (middle) and the DTMB5415 model (bottom) approximated via 7,562 (Wigley), 11,542 (S60) and 12,586 (DTMB5415) flat triangular panels.

and A^H denotes the wetted area of the ship hull surface Σ^H. The kinematic viscosity ν is taken as $1.14\times10^{-6} m^2/s$ hereafter. The form factor k is estimated via the relation

$$k = 0.6\sqrt{\Delta/L^3} + 9\Delta/L^3 \quad \text{with} \quad 0.05 \le k \le 0.40 \qquad (11c)$$

given in Manen and Oossanen (1988). Here, Δ denotes the displacement of the ship.

The roughness correction C^a in (10) is determined via the Bowden-Davison formula

$$C^a = 10^{-4}\,\frac{A^H}{2L^2}\,R \quad \text{where} \qquad (12a)$$

$$4 \le R \equiv 1050\,(k_s/L)^{1/3} - 6.4 \le 8 \qquad (12b)$$

given in Bowden and Davison (1974). Here, k_s characterizes the hull roughness. The standard value

$$k_s = 0.00015\text{m} \qquad (12c)$$

is used in Ma et al. (2016b).

The wave drag coefficient C^w is determined via integration of the pressure p at the hull surface Σ^H, i.e.

$$C^w = \int_{\Sigma^H} n^x p\, da \qquad (13)$$

where p is given by the Bernoulli relation (5d). The Neumann-Michell theory is used to compute the flow around the ship hull surface Σ^H and the related pressure p. Expression (13) for C^w shows that the parallel midbody and the bottom of a ship hull surface, where $n^x \approx 0$, contribute little to the wave drag, which mostly stems from the upper parts of the bow and stern regions where $n^x \neq 0$. The drag of a ship can therefore be expected to be much more sensitive to the precise position of the ship hull than the sinkage and the trim, which are mostly determined by the pressure distribution over the hull bottom as noted earlier.

A_0^H, A_1^H and A_a^H denote the wetted areas of the hull surfaces Σ_0^H of the ship at rest or the hull surfaces Σ_1^H or Σ_a^H determined from the sinkage and the trim predicted by the numerical approach or the experimental approach considered in sections 3 and 4. Expression (11b) shows that differences among the wetted areas A_0^H, A_1^H and A_a^H yield differences among the friction drag coefficient C^f. The total drag coefficients C_0^t, C_1^t, C_a^t, the viscous drag coefficients C_0^v, C_1^v, C_a^v and the wave drag coefficents C_0^w, C_1^w, C_a^w correspond to the hull surfaces Σ_0^H, Σ_1^H or Σ_a^H, respectively.

6. Illustrative applications for three ship models

The simple methods for determining the sinkage, the trim and the drag of a freely-floating ship given above are now applied to three ship models: the Wigley hull, the S60 model and the DTMB5415 model. The length L of these ship models is 2.5m for the Wigley hull, 4m for the S60 model and 5.72m for the DTMB5415 model. Side and bottom views of the wetted hull surfaces Σ_0^H for these three ship models are shown in Fig.6. Half of the hull surface Σ_0^H is approximated via 7562, 11,542 or 12,586 flat triangular panels for the Wigley hull, the S60 model and the DTMB5415 model, respectively.

Fig.7 depicts the midship sinkage H^m/D and the trim sinkage H^τ/D for the three ship models at Froude numbers $0.1 \le F \le 0.45$. The numerical predictions given by (5) with the Neumann-Michell theory applied to the hull surfaces Σ_0^H or Σ_1^H are depicted together with experimental measurements and the predictions given by the

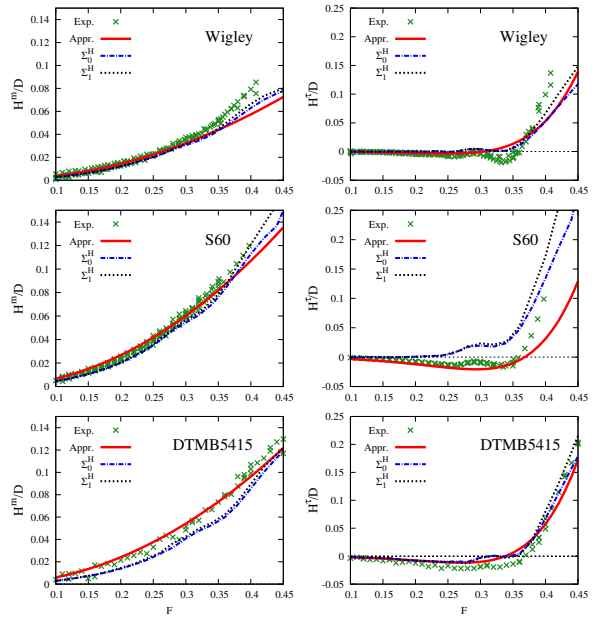

Figure 7: The midship sinkage H^m/D (left) and the trim sinkage H^τ/D (right) for the Wigley hull (top), the Series 60 model (center) and the DTMB5415 model (bottom). Experimental measurements (Exp.) are shown together with the predictions given by the analytical relations (8) obtained from an analysis of experimental measurements (Appr.) and the numerical predictions given by the Neumann-Michell theory applied to the hull surfaces Σ_0^H or Σ_1^H.

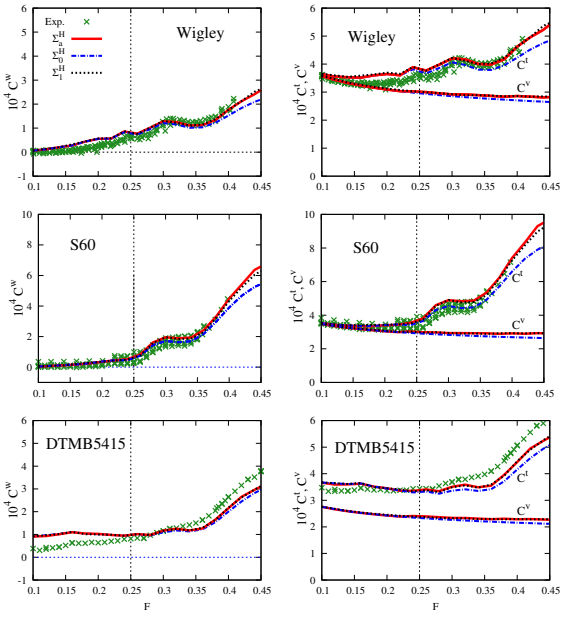

Figure 8: The left side depicts the wave drag C^w and the right side depicts the viscous drag C^v and the total drag C^t for the Wigley hull (top), the S60 model (center) and the DTMB5415 model (bottom). Experimental measurements (Exp.) are shown together with the theoretical predictions (10)-(13) applied to the hull surfaces Σ_a^H, Σ_0^H or Σ_1^H.

simple analytical relations (8) obtained from an analysis of experimental measurements.

Fig.7 shows that the numerical predictions for the hull surfaces Σ_0^H or Σ_1^H are very close for the midship sinkage H^m, and do not differ significantly for the trim sinkage H^τ. Moreover, these numerical predictions are in relatively good agreement with the experimental measurements. The numerical predictions for the hull surface Σ_1^H are not closer to the experimental measurements of the trim sinkage H^τ than the numerical predictions for the hull surface Σ_0^H. This finding suggests that it is sufficient to compute the flow around the 'static' ship hull surface Σ_0^H, instead of the 'dynamic' hull surface Σ_1^H, for the purpose of predicting the sinkage and the trim of common monohull ships at Froude numbers $F \leq 0.45$. Fig.7 also shows that the simple analytical relations (8) yield predictions of the midship sinkage H^m and the trim sinkage H^τ that are in relatively good agreement with the numerical predictions, as well as the experimental measurements.

Fig.8 depicts the theoretical predictions of the total drag C^t, the wave drag C^w and the viscous drag C^v that correspond to the hull surfaces Σ_0^H, Σ_1^H and Σ_a^H for the Wigley hull, the S60 model and the DTMB5415 model. The experimental measurements C_e^t of the total drag C^t that are also shown in Fig.8 correspond to freely-floating ship models, and are determined as in Longo and Stern (1998) via the relation

$$C_e^t = C^r + C_0^v \tag{14}$$

where C^r denotes the residual drag of the freely-floating ship model and C_0^v is the viscous drag of the hull surface Σ_0^H of the ship at rest.

Fig.8 shows that differences among the theoretical drag coefficients C^t, C^w and C^v for the hull surfaces Σ_1^H and Σ_a^H are practically negligible; i.e. the drag coefficients for the hull surface Σ_a^H defined by the simple analytical relations (8) and the hull surface Σ_1^H obtained via potential flow computations for the hull surface Σ_0^H of the ship at rest are nearly identical. Moreover, the total drags C^t of the hull surfaces Σ_1^H and Σ_a^H are in reasonable overall agreement with the experimental measurements C_e^t. Fig.8 also shows that differences between the theoretical drag coefficients C^t, C^w, C^v for the hull surfaces Σ_1^H or Σ_a^H and the hull surface Σ_0^H of the ship at rest are fairly small for $F < 0.25$, but increase rapidly for $0.25 < F$. Sinkage and trim effects on the drag can then be ignored for $F < 0.25$, but can be significant for $0.25 < F$.

Experimental measurements, denoted as C_e^t, of the total drag C^t for a freely-floating ship are now compared to the corresponding theoretical predictions C_0^t or C_1^t for the ship hull surfaces Σ_0^H or Σ_1^H. The relative differences between the experimental measurements C_e^t and the corresponding theoretical predictions C_0^t or C_1^t for the ship hull surfaces Σ_0^H or Σ_1^H are given by

$$e_0^t = (C_e^t - C_0^t)/C_0^t \quad \text{and} \quad e_1^t = (C_e^t - C_1^t)/C_1^t \tag{15}$$

The relative errors e_0^t and e_1^t are associated with the hull surface Σ_0^H, which ignores sinkage and trim, or the hull surface Σ_1^H that accounts for the influence of sinkage and trim on the drag. Thus, the errors e_0^t and e_1^t provide a basis for validating the simple theoretical method considered here to account for the influence of sinkage and trim on the drag of a freely-floating ship.

Fig.9 depicts the relative errors e_0^t and e_1^t for the Wigley, S60 and DTMB5415 models at Froude numbers within the range $0.25 \leq F \leq 0.45$ for which sinkage and trim have a significant influence on the drag. The dashed

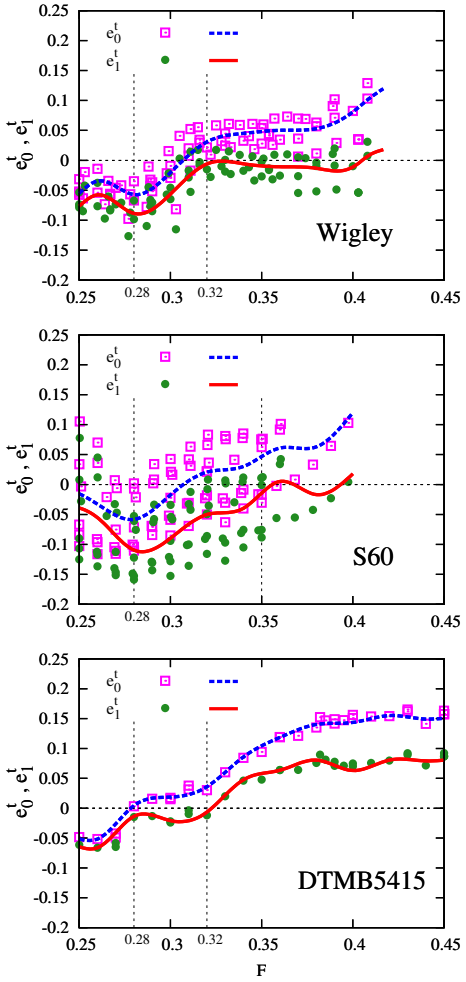

Figure 9: Relative errors e_0^t and e_1^t, and corresponding smoothing spline fits, between experimental measurements of the total drag C^t and theoretical predictions for the hull surface Σ_0^H of a ship at rest or the hull surface Σ_1^H that accounts for sinkage and trim effects.

and solid lines in Fig.9 are smoothing spline fits that correspond to the experimental values of e_0^t (squares) or e_1^t (circles). The errors e_0^t increase for $0.28 < F$ and are significant for $0.35 < F$. Indeed, the errors e_0^t are larger than 10% for $0.4 < F$. The errors e_1^t are much smaller than the errors e_0^t for the Wigley hull and the DTMB5415 model at $0.32 < F$, and for the S60 model at $0.35 < F$. Specifically, the errors e_1^t vary within $\pm 2\%$ for the Wigley and S60 models in the Froude number ranges $0.32 < F$ or $0.35 < F$, and are smaller than about 7% for the DTMB5415 model at $0.32 < F$. The relatively large errors for the DTMB5415 model might stem from the fact that this model has a transom stern, as shown in Fig.1, that is ignored here.

7. Conclusion

The influence of sinkage and trim on the drag of a typical freely floating monohull ship has been considered. The comparisons of experimental measurements and theoretical computations reported for the Wigley, S60 and DTMB5415 models suggest that the sinkage and the trim experienced by common monohull ships are small, and have limited influence on the drag, for Froude numbers F smaller than about 0.25. However, the sinkage and the trim, and their influence on the drag, increase rapidly for $0.25 < F$, and are significant for the highest value $F = 0.45$ of the Froude number range $0.1 \leq F \leq 0.45$ considered here. E.g., the theoretical predictions given in Ma et al. (2016b) show that at $F = 0.45$, the Wigley hull and the S60 model experience an increase in drag of about 15%, and the drag of the DTMB5415 model is about 7% higher, due to sinkage and trim effects. The influence of sinkage and trim on the drag (especially the wave drag) of a ship can then be significant, and moreover depends on the hull form. Sinkage and trim effects should then be considered within the design process, arguably even at early design stages and for hull form optimization.

Accordingly, practical methods suited for routine applications to ship design have been considered here to determine the sinkage, the trim and the drag. Specifically, the sinkage and the trim are determined via two simple alternative methods. These two methods yield predictions of sinkage and trim that do not differ greatly, and moreover are in reasonable agreement with experimental measurements for a broad class of monohull ships. The drag is similarly evaluated in a simple way, based on the classical Froude decomposition into viscous and wave components.

One of the two simple alternative methods considered to determine the sinkage and the trim is a numerical method. This method only involves linear potential flow computations (the Neumann-Michell theory is used) for the wetted hull surface Σ_0^H of the ship at rest. Indeed, numerical predictions of sinkage and trim for the 'static' hull surface Σ_0^H of the ship at rest and for the 'dynamic' hull surface Σ_1^H, which is determined from flow computations for the hull surface Σ_0^H and thus accounts for the hull sinkage and trim, do not differ significantly for the Wigley, S60 and DTMB5415 models. The sinkage and the trim of common monohull ships at $F \leq 0.45$ can then be predicted without iterative flow computations for a sequence of ship hull surfaces Σ_n^H. This notable simplification stems from the fact that the sinkage and the trim are primarily determined by the pressure distribution over the bottom of the ship hull surface, and therefore are not highly sensitive to the precise position of the ship.

The other method considered to determine the sinkage and the trim is based on an analysis of experimental measurements (for 22 ship models). This alternative method yields explicit analytical relations for the sinkage and the trim, and thus requires no flow computations. Specifically, the relations (8) explicitly determine the sinkage and the trim of a ship in terms of the ship speed V and four basic parameters (the length L, the beam B, the draft D, and the block coefficient C_b) that characterize the ship geometry.

As already noted, the drag is also estimated in a simple way, based on the classical Froude decomposition of the drag into viscous and wave components. Specifi-

cally, classical semiempirical expressions for the friction drag, the viscous drag and the drag due to hull roughness are used, and the wave drag is evaluated via a linear potential flow method (the Neumann-Michell theory). This simple approach can be applied to ship models as well as full-scale ships with smooth or rough hull surfaces.

The wave drag is largely determined by the pressure distribution at the bow and the stern of a ship, and is then much more sensitive to the precise position of the ship hull than the sinkage and the trim, which are mostly determined by the pressure at the hull bottom as already noted. This basic difference explains why the sinkage and the trim of a ship can be realistically estimated from flow computations around the hull surface Σ_0^H of the ship at rest, whereas the drag must be evaluated for a 'dynamic' ship hull surface Σ_{st}^H that accounts for the sinkage and the trim experienced by the ship.

However, the hull surface Σ_{st}^H does not need to be very precise. Indeed, a main result of the numerical computations reported here for the Wigley hull and the S60 and DTMB5415 models is that the hull surface Σ_a^H defined by the explicit analytical relations (8) and the hull surface Σ_1^H determined from potential flow computations for the hull surface Σ_0^H of the ship at rest have nearly identical drag coefficients C^t. Another notable result is that the (nearly identical) predictions of the drag for the ship hull surfaces Σ_a^H or Σ_1^H, which correspond to the sinkage and the trim predicted by the explicit analytical relations (8) or via flow computations for the hull surface Σ_0^H as already noted, are significantly higher than the drag predicted for the hull surface Σ_0^H of the ship at rest.

Moreover, and more importantly for practical applications, the drag coefficients predicted for the hull surfaces Σ_a^H or Σ_1^H are much closer to experimental measurements than the drag of the hull surface Σ_0^H of the ship at rest for the Wigley hull and the S60 and DTMB5415 models at Froude numbers for which sinkage and trim effects are significant. Specifically, Fig.9 shows that, at Froude numbers greater than about 0.32 to 0.35 for which sinkage and trim effects are large, the relative errors e_1^t between experimental measurements of the total drag and theoretical drag predictions for the hull surface Σ_1^H, which accounts for the sinkage and the trim as already noted, are significantly smaller than the errors e_0^t associated with predictions for the hull surface Σ_0^H of the ship at rest.

This finding provides a partial validation of the simple approach considered here, and suggests that the influence of sinkage and trim on the drag of a freely floating monohull ship at $F \leq 0.45$ can be determined in a very simple way that is well suited for routine applications to design, including at early stages and for optimization. In particular, if the analytical relations (8) are used to estimate the sinkage and the trim, prediction of the drag of a freely floating ship only requires a computation of the flow around the hull Σ_a^H, i.e., a single (linear potential) flow computation per Froude number.

As is noted in the introduction, the drag of a freely floating ship is influenced by sinkage and trim, considered in the study, as well as by several more complicated flow features that are not considered here. These additional features include flow separation that typically occurs at a ship stern, notably a transom stern, and wave-breaking at a ship bow. For the Wigley and S60 models, these additional complications only have a relatively minor influence on the drag. Accordingly, Fig.9 shows that the relative errors e_1^t between experimental measurements of the total drag and theoretical predictions for the hull surface Σ_1^H are quite small, indeed vary within $\pm 2\%$, for these two models at Froude numbers (greater than about 0.32 to 0.35) for which sinkage and trim effects are large. The errors e_1^t are appreciably larger (as large as 7%) for the DTMB5415 model, possibly because this ship model has a transom stern.

In any case, for the three ship models considered here, the errors e_1^t are much smaller than the errors e_0^t associated with drag predictions for the hull surface Σ_0^H of the ship at rest for Froude numbers (greater than about 0.35) for which sinkage and trim effects are significant. A large part of the errors between theoretical predictions and experimental measurements of the drag of a floating ship may then be attributed to sinkage and trim effects. Moreover, these errors can be accounted for in a practical way, as already noted.

References

Bowden, B.S., Davison, N.J., 1974. Resistance increments due to hull roughness associated with form factor extrapolation methods. National Physical Laboratory NP Ship Technical Manual. NPL Ship Report TM 3800, 1974.

Broglia, R., Bouscasse, B., Jacob, B., Olivieri, A., Zaghi, S., & Stern, F., 2011. Calm water and seakeeping investigation for a fast catamaran. 11th international conference on fast sea transportation (FAST2011), Honolulu, Hawaii.

Broglia, R., Jacob, B., Zaghi, S., Stern, F., & Olivieri, A., 2014. Experimental investigation of interference effects for high-speed catamarans. Ocean Engineering, 76, 75-85.

Chen, X., Zhu, R., Ma, C., Fan, J., 2016. Computations of linear and nonlinear ship waves by higher-order boundary element method. Ocean Engineering, 114, 142-153.

Cook, S. S., 2011. Effects of headwinds on towing tank resistance and PMM tests for ONR Tumblehome. Univ. of Iowa

Cusanelli, D. S., 2007. Joint high speed sealift (JHSS) baseline shaft & strut (model 5653) series 1: bare hull resistance, appended resistance, and alternative bow evaluations. Naval Surface Warfare Center Carderock Div Bethesda MD.

Doctors, L. J., 2015. Hydrodynamics of High-Performance Marine Vessels, CreateSpace Independent Publishing Platform, 1 edition.

Fu, T., Karion, A., Pence, A., Rice, J., Walker, D., Ratcliffe, T., 2005. Characterization of the Steady Wave Field of the High Speed Transom Stern Ship-Model 5365 hull-shape. Naval Surface Warfare Center Carderock Div Bethesda MD.

He, W., Castiglione, T., Kandasamy, M., Stern, F., 2015. Numerical analysis of the interference effects on resistance, sinkage and trim of a fast catamaran. Journal of Marine Science and Technology, 20(2), 292-308.

Huang, F., Yang, C., Noblesse, F., 2013. Numerical implementation and validation of the Neumann-Michell theory of ship waves. European Journal of Mechanics-B/Fluids, 42, 47-68.

Kajitani, H., Miyata, H., Ikehata, M., Tanaka, H., Adachi, H., Namimatsu, M., Ogiwara, S., 1983. The summary of the cooperative experiment on Wigley parabolic model in Japan. Tokyo Univ. (JAPAN).

Longo, J., Stern, F., 1998. Resistance, sinkage and trim, wave profile, and nominal wake tests and uncertainty assessment for DTMB

model 5512. In Proc 25th American Towing Tank Conference, Iowa.

Ma, C., Zhang, C., Chen, X., Jiang, Y., Noblesse, F., 2016a. Practical estimation of sinkage and trim for commmon generic monohull ships. Ocean Engineering, 126, 203-216.

Ma, C., Zhang, C., Huang, F., Yang, C., Gu, X., Li, W., Noblesse, F., 2016b. Practical evaluation of sinkage and trim effects on the drag for common generic freely floating monohull ships. Submitted.

Manen, J.D., Oossanen, P., 1988. Principles of Naval Architecture: Resistance and Propulsion, Vol. 2. New Jersey: SNAME.

McCarthy, J. H., 1985. Collected experimental resistance component and flow data for three surface ship model hulls. David W Taylor Naval Ship Research and Development Center Bethesda MD.

Molland, A. F., Wellicome, J. F., Couser, P. R., 1994. Resistance experiments on a systematic series of high speed displacement catamaran forms: variation of length-displacement ratio and breadth-draught ratio. University of Southampton, Ship Science Report, No.71.

Molland, A. F., Lee, A. R., 1995. Resistance experiments on a series of high speed displacement catamaran forms: variation of prismatic coefficient. University of Southampton, Ship Science Report, No.86.

Ni, C.B., Zhu, R.C., Miao, G.P., Fan, J., 2011. Hull gesture and resistance prediction of high-speed vessels. Journal of Hydrodynamics, Ser.B, 23(2), 234-240.

Noblesse, F., Huang, F., & Yang, C., 2013a. The Neumann-Michell theory of ship waves. Journal of Engineering Mathematics, 79(1), 51-71.

Noblesse, F., Huang, F., Yang, C., 2013b. Evaluation of ship waves at the free surface and removal of short waves. European Journal of Mechanics-B/Fluids, 38, 22-37.

Olivieri, A., Pistani, F., Avanzini, A., Stern, F., Penna, R., 2011. Towing tank experiments of resistance, sinkage and trim, boundary layer, wake, and free surface flow around a naval combatant INSEAN 2340 model. Iowa Univ. Iowa City Coll of Engineering.

Souto-Iglesias, A., Fernández-Gutiérrez, D., Pérez-Rojas, L., 2012. Experimental assessment of interference resistance for a Series 60 catamaran in free and fixed trim-sinkage conditions. Ocean Engineering, 53, 38-47.

Subramani, A.K., Paterson, E. G., Stern, F., 2000. CFD calculation of sinkage and trim. Journal of ship research, 44(1), 59-82.

Yang, C., Huang, F., Noblesse, F., 2013. Practical evaluation of the drag of a ship for design and optimization. Journal of Hydrodynamics, Ser. B, 25(5), 645-654.

Yang, C., Kim, H.Y., Noblesse, F., 2007. A practical method for evaluating steady flow about a ship, 9^{th} Il Conf. on Fast Sea Transportation, Shanghai China

Yang, C., & Löhner, R., 2002. Calculation of ship sinkage and trim using a finite element method and unstructured grids. International Journal of Computational Fluid Dynamics, 16(3), 217-227.

Yang, C., Löhner, R., Noblesse, F., & Huang, T. T., 2000. Calculation of ship sinkage and trim using unstructured grids. In European Congress on Computational Methods in Applied Sciences and Engineering, ECCOMAS.

Yao, C.B., Dong, W. C., 2012. A Method to Calculate Resistance of Ship Taking the Effect of Dynamic Sinkage and Trim and Viscosity of Fluid. In Applied Mechanics and Materials, Trans Tech Publications, 121, 1849-1857.